3 CHALLENGES FOR A NEW 1KM NON–HYDROSTATIC MODEL OVER THE ALPINE AREA

Guy de Morsier*, Oliver Fuhrer and Marco Arpagaus
Federal Office of Meteorology and Climatology, MeteoSwiss, Zurich, Switzerland

1. INTRODUCTION

The Swiss meteorological office (MeteoSwiss) is planning to run the COSMO model (Steppeler et al. 2003, Doms and Förstner 2003, Doms and Schättler 2002, Baldauf et al. 2011) with an O (1 km) mesh-size on an operational basis. To attain this goal the actual dynamical core of the model must be made numerically stable for an increased steepness of the orography. Moreover it should provide accurate forecasts with a minimally filtered orography. The right balance between this filtering and the usage of some horizontal (numerical) diffusion needs to be found. This paper shows the general setup of the model and to some extent how much can be exploited from the increased horizontal (and vertical) resolution.

2. SETUP OF THE COSMO-1 MODEL

The model is based on the primitive hydro-thermo-dynamical equations describing compressible non-hydrostatic flow in a moist atmosphere without any scale approximations. To reduce numerical errors an hydrostatic time-independent dry atmosphere (basic state at rest with exponential and asymptotic isothermal profile in the stratosphere) is subtracted from these equations. The prognostic variables are the pressure, the three wind components, temperature, specific humidity, cloud water, cloud ice, graupel, rain, snow and turbulent kinetic energy (TKE). The wind components follow the Arakawa-C staggering and a rotated lat/lon grid is used. More details can be found under http://www.cosmo-model.org/

The vertical levels are shown in Fig. 1 and are obtained from the height-based terrain-following coordinate modified by a vertical decay of the topographic signature with height from Leuenberger et al. 2010. We use a quadratic distribution of the 80 levels and a Lorenz staggering. This generalization of the SLEVE vertical coordinate system (SLEVE2) enables an almost uniform thickness of the lowermost computational layers. This is illustrated by the minimum layer thicknesses shown on Fig. 1.

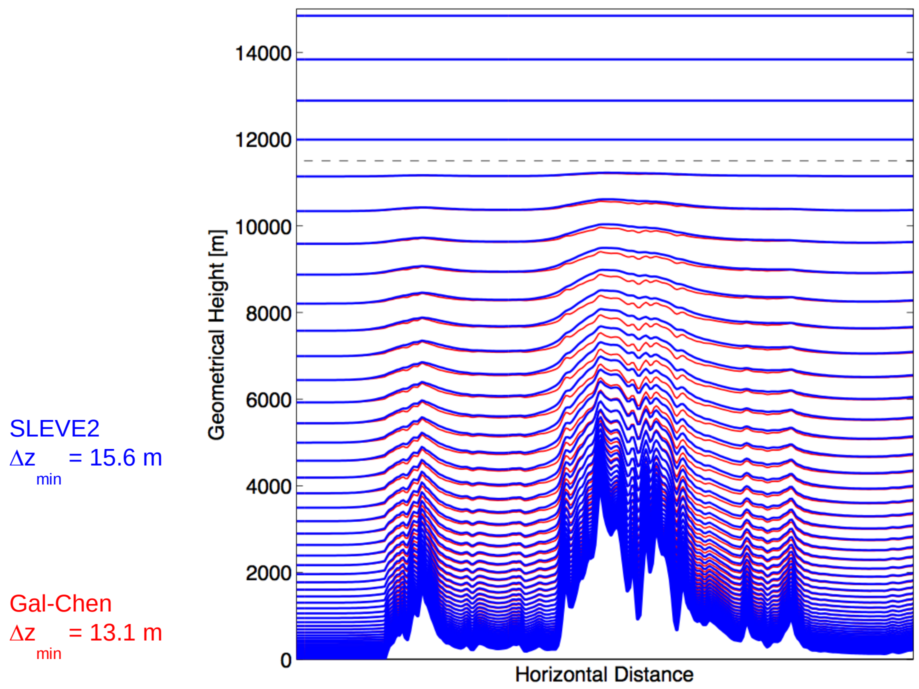

Fig. 1 Vertical cross-section of part of the 80 levels used by the model in blue (top at 22 km). These height-based vertical levels follow the generalized terrain-following SLEVE2 coordinate system. The red lines show the usual Gal-Chen coordinate system.

* *Corresponding author address:* Guy de Morsier, MeteoSchweiz, PO box, CH-8044 Zürich; guy.demorsier@meteoswiss.ch

The computational domain covers the whole Alpine range and uses an horizontal resolution of a hundredth of a degree (1.1 km). Fig. 2 illustrates the size of the domain and the extent of the 1-way nesting Davies-type lateral boundary relaxation zone.

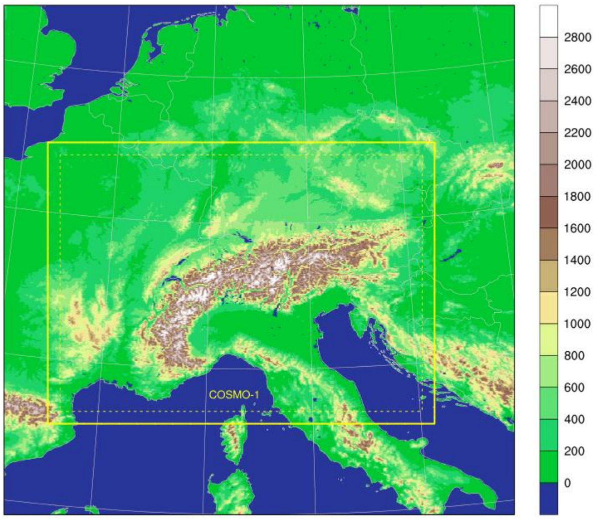

Fig. 2 Computational domain of 1181 x 861 km^2 (1062 x 774 grid points, full yellow line) with an horizontal resolution of $\Delta\lambda = \Delta\phi = 0.01°$ (1.1 km) and relaxation zone of 35 km (32 grid points) as stippled yellow line.

Orographic filtering (Fig. 3) removes from the original 1 km GLOBE data all waves with a wavelength smaller than 4 Δx waves and locally regions with grid point height differences exceeding 750 m steps such that the maximum slope of the orography does not exceed 36° (Fig. 4).

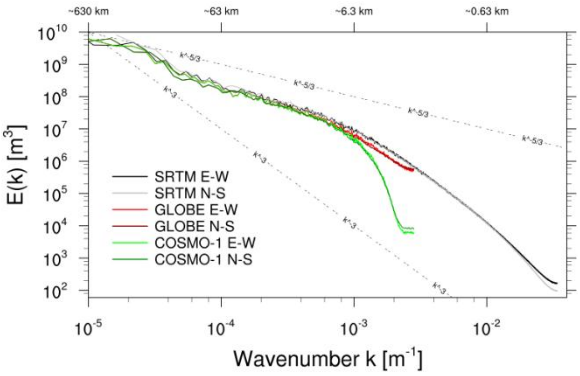

Fig. 3 Spectral energy densities computed from the orography of the model (COSMO-1) and from the unfiltered GLOBE 1 km data (mean East-West and North-South components). Shuttle data (SRTM) at full resolution is included for comparison.

2.1 *Dynamical settings*

The numerical integration follows the 2-timelevel horizontally explicit, vertically implicit time-split scheme with a 3^{rd} -order Runge-Kutta time discretization (Δt = 10 s). The spatial discretization uses explicit

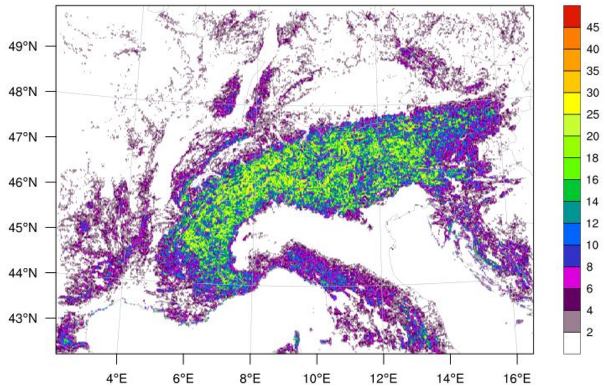

Fig. 4 Maximum of the 4 finite difference gradients in x- and y-direction in degrees (max. 36°).

5^{th}-order advection in the horizontal direction and 2^{nd}-order implicit vertical advection. Above 11km Rayleigh damping is applied to the upper layers. Horizontal non-linear Smagorinsky diffusion (Baldauf et al. 2012) is used instead of artificial hyper-diffusion. In the fast waves solver (split time steps) a 2D divergence damping (off-centering in the vertical) helps to keep the dynamical core stable. For idealized cases, this solver can cope with slopes up to 45° (Baldauf 2012).

2.2 *Physical settings*

The subgrid-scale turbulence is parameterized by a prognostic TKE closure at level 2.5 including effects from subgrid-scale condensation and from thermal circulations. The surface layer parameterization follows a scheme based on TKE including a laminar-turbulent roughness layer. Cloud water condensation and evaporation is obtained by saturation adjustment and precipitation is formed by a bulk microphysics parameterization including water vapour, cloud water, cloud ice, rain, snow and graupel with 3D transport for the precipitating phases. No parameterization of deep convection is employed but a reduced Tiedtke (1989) scheme allows for shallow convection. The radiation scheme follows Ritter and Geleyn (1992) and is called every 6 minutes. The parameterization of the subgrid-scale orographic drag is switched off.

3. RELATED QUESTIONS

Apart from the numerical errors associated with the calculation of the pressure gradient forces in case of steeply sloping coordinate surfaces, the overall stability of the dynamical core can be limited by the occurrence of horizontal shear instabilities. In this case, the purely vertically acting turbulent scheme has no stabilizing effect. Instead of using selective non-linear Smagorinsky diffusion (with a very small dimensionless diffusion coefficient of 0.03, see Baldauf et al. 2012) a 3D Smagorinsky-Lilly (1962, 1963) type turbulence closure could be used. This has been done for the COSMO model by Langhans et al. (2012) and was tested for the neutral and the convective boundary layer (CBL). But this approach still needs to be tested on steep terrains and its results verified with respect to the initiation and development of resolved deep convection.

4. RESULTS

Models run at a higher resolution compared to operational (6.6 km and 2.2 km) have a potential for a better orographic forcing. As an example we take a spring convection case where the triggering mechanism on the Southern side of the Alps was very sensitive to the resolution.

In Fig. 5 the operational 6.6 km model shows the 24h forecasted total precipitation. To the NW of Switzerland a large band of weak rain is present and at the foothills of the Alpine and Apennine orography ranges a more convective and intense precipitation occurs. A similar pattern is found in the 24h cumulated radar composite (Fig. 8) but the weak rain reaches the NW Swiss border and the most intense precipitation is NE of Génova.

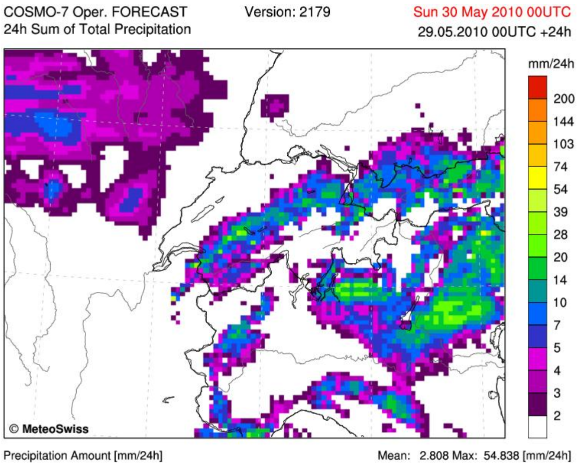

Fig. 5 Total precipitation from the operational COSMO model with a resolution of 6.6km.

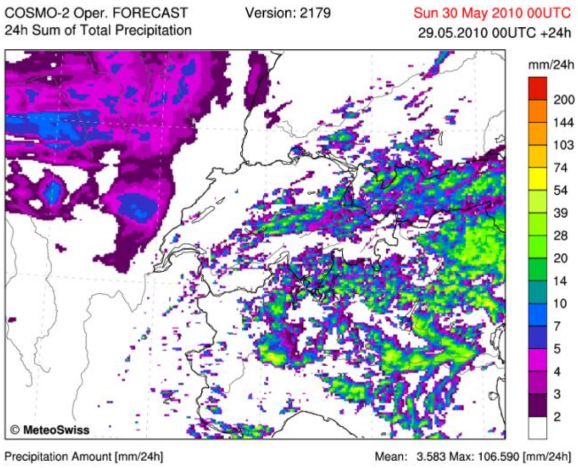

Fig. 6 Total precipitation from the operational COSMO model with a resolution of 2.2 km.

In the operational 2.2 km model the weak rain NW of Switzerland and the rain at the foothills in-

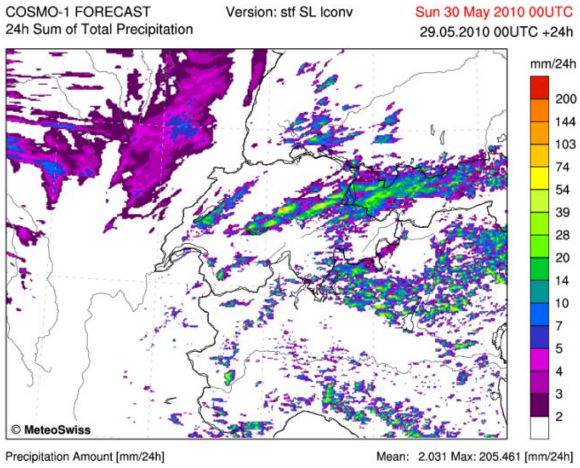

Fig. 7 Total precipitation from the COSMO model with a resolution of 1.1km and all the settings described in this contribution.

creases (Fig. 6) but very little rain is close to the NW Swiss border. On the other side of the Alps the rain along the Pô river is very much exaggerated. For the COSMO-1 simulation (Fig. 7) much less rain occurs on the NW corner and the rain along the Pô river nearly vanishes. Except for the convective cell NE of Génova this picture corresponds better to the radar measurements although the visibility of the radar along the Eastern side of the domain is probably very limited.

The main difference between the 1.1 km and 2.2 km simulations (except the different horizontal and vertical resolutions; COSMO-2 has only 60 vertical levels) is the advection of the humidity variables. For COSMO-2 the direction splitted 2nd order Bott scheme is used while in the COSMO-1 case a semi-Lagrangian (SL) scheme with tri-cubic interpolation takes advantage that it computes the interpolation in 3D in one step, therefore no splitting error occurs.

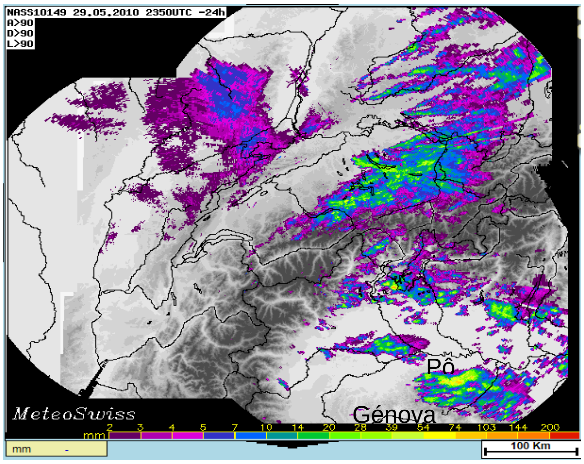

Fig. 8 Cumulated total precipitation summed up over the 24h of May 29, 2010 from the 3 Swiss radar stations (Albis, Dôle and Lema).

7. CONCLUSIONS AND OUTLOOK

The potential of high resolution runs was illustrated in the light of a convective case study and some of the questions related to the setup of the model were mentioned.

More connections between the simulated flows regarding the non-linear scale interactions and the non-linear forcings should be analysed and the structure of the CBL should be compared to measurements so that the benefit of the higher vertical resolution can be demonstrated.

6. REFERENCES

Baldauf, M., 2012: Development of a new fast waves solver for the Runge-Kutta scheme, *COSMO/CLM User Seminar*, Offenbach 6-8 March, Germany, [available online at http://www.dwd.de].

Baldauf, M., G. Zängl, 2012: Horizontal nonlinear Smagorinsky diffusion. *COSMO newsletter*, **12**, 3-7, [available online at: http://www.cosmo-model.org].

Baldauf, M., A. Seifert, J. Förstner, D. Majewski and M. Raschendorfer, 2011: Operational convective-scale numerical weather prediction with the COSMO model: description and sensitivities. *Mon. Wea. Rev*., **139**, 3887–3905.

Doms, G. and U. Schättler, 2002: A Description of the Nonhydrostatic Regional Model LM. Part I: Dynamics and Numerics. [Available online at http://www.cosmo-mode.org/].

Doms, G. and J. Förstner, 2003: Development of a kilometer-scale NWP-system: LMK. COSMO Newsletter, 4, 159-167. [Available online at http://www.cosmo-model.org/].

Langhans,W., J. Schmidli, and B. Szintai, 2012: A Smagorinsky-Lilly turbulence closure for COSMO-LES: Implementation and comparison to ARPS. *COSMO newsletter*, **12**, 20-31.

Leuenberger, D., M. Koller, O. Fuhrer, and C. Schär, 2010: A generalization of the SLEVE vertical coordinate. *Mon. Wea. Rev*., **138**, 3683–3689.

Steppeler, J., et al., 2003: Meso-gamma scale forecasts using the non-hydrostatic model LM. *Meteor. Atmos. Phys*., **82**, 75–96.